nature communications

Article

https://doi.org/10.1038/s41467-025-68073-w

Modular assembly of chiral amino acid derivatives and peptides from commonly available feedstocks

Received: 14 September 2025

Accepted: 16 December 2025

Published online: 30 December 2025

Check for updates

Wei-Wei Ding[1], Zhi-Yuan He[1], Wan-Yu Wang[1], Zhi-Yong Han[1,2] & Liu-Zhu Gong[1,2]

α-Amino acids are fundamental components of proteins and natural molecules, with non-natural variants highly valued in both academia and industry for their ability to tune chemical, physical, and pharmaceutical properties. Herein, we report a photoredox-catalyzed protocol for the synthesis of optically active α-amino amides from readily available aldehydes, amines, and formamides. A dual catalytic system combining a chiral sodium phosphate with tetrabutylammonium decatungstate (TBADT) under visible light enables this transformation. The process achieves high enantioselectivity and allows two-step conversion to free amino acids without significant racemization. Consequently, diverse, synthetically useful structures—including β-branched and α,β-diamino acid derivatives, glycosylated amino acids, isotopically labeled compounds (deuterium and ^{15}N), and peptides—have been rapidly constructed. Flow chemistry further broadens substrate tolerance and eliminates prefunctionalization steps. Here, we show that leveraging TBADT-driven carbamoyl radical generation and chiral catalysis provides a practical route to diverse chiral scaffolds, thereby advancing peptide synthesis and drug discovery.

Amino acids serve as fundamental building blocks in nature, constituting core structural motifs of proteins and numerous other biologically important molecules (Fig. 1a)[1–5]. Beyond their natural functions, amino acids and their derivatives—particularly non-proteinogenic variants—have gained increasing importance in pharmaceutical development, material science, and asymmetric catalysis[6]. The recent surge in peptide-based therapeutics, accelerated by advances in screening technologies like mRNA display, has intensified the demand for structurally diverse amino acids with precise stereochemical control[7]. This technology enables the incorporation of non-natural amino acids into vast peptide libraries, significantly expanding the structural and functional diversity of potential drug candidates[8]. Consequently, developing efficient, scalable, and economical methods for synthesizing enantiomerically pure amino acids from readily available precursors has become increasingly urgent for advancing peptide drug discovery and development[9]. Traditional approaches to synthesizing chiral α-amino acids rely predominantly on polar/heterolytic processes[10]. These include asymmetric hydrogenations of dehydroamino acids[11] or α-imino esters[12,13], electrophilic aminations of enolates[14], alkylations of glycine derivatives via phase-transfer catalysis[15] and through Pd/Cu synergistic catalytic systems[16,17], and nucleophilic additions to α-imino esters[18]. More recent advances include asymmetric Ugi-type multicomponent reactions, which are highly valuable but involve odorous and toxic isocyanides[19]. Other developments involve stereocontrolled 1,3-nitrogen migration via metal-catalyzed nitrene insertion that relies on activated nitrogen sources[20,21].

In recent years, radical-based methods[22,23] have emerged as promising alternatives for asymmetric amino acid synthesis. Notably, nickel-catalyzed enantioconvergent cross-coupling of racemic α-

[1]Hefei National Laboratory for Physical Sciences at the Microscale and Department of Chemistry, University of Science and Technology of China, Hefei, China. [2]Department of Chemistry, University of Science and Technology of China, Hefei, China. e-mail: hanzy2014@ustc.edu.cn; gonglz@ustc.edu.cn

https://doi.org/10.1038/s41467-025-68073-w

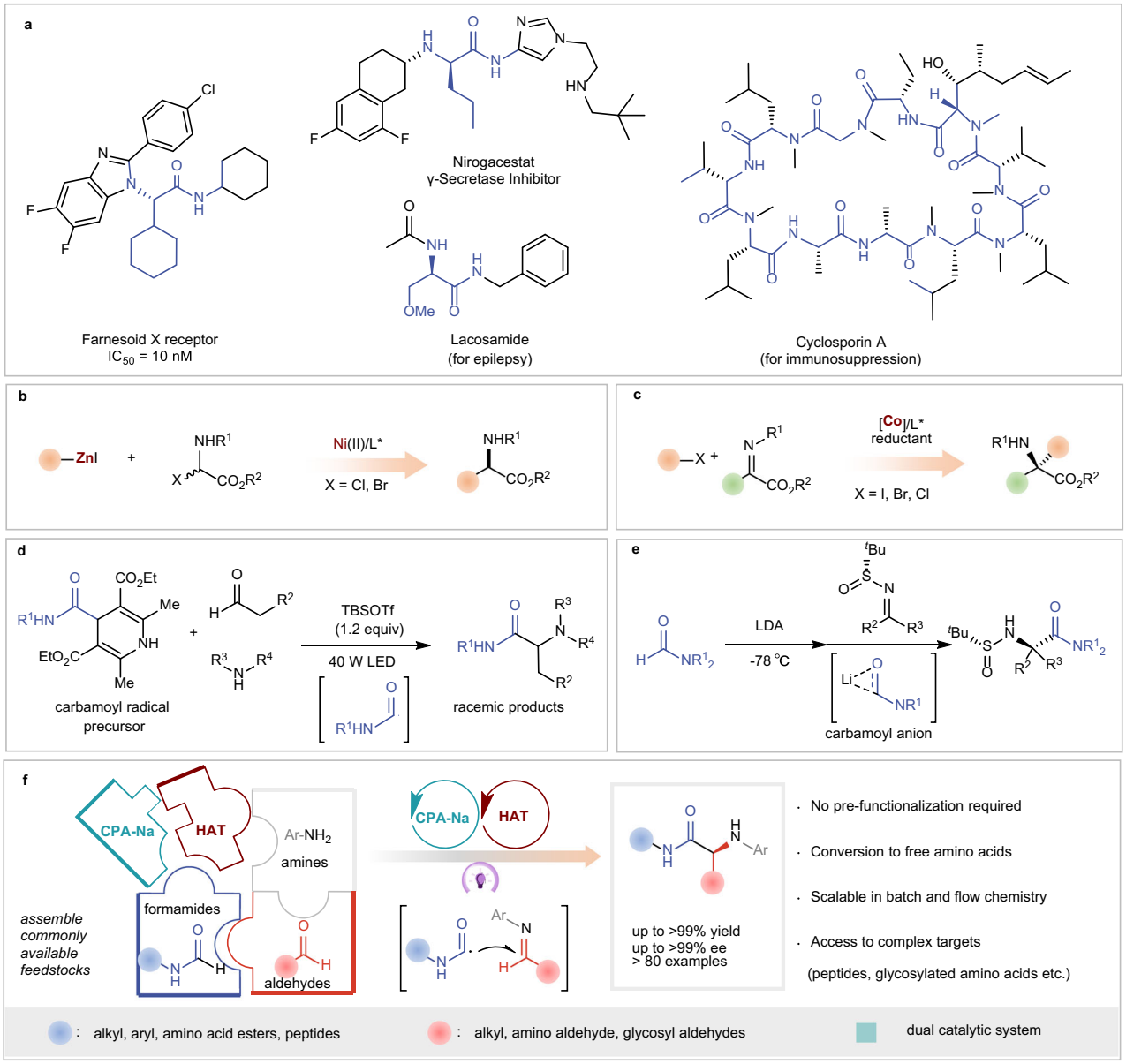

Fig. 1 | Bioactive chiral amino acid derivatives and synthetic approaches. **a** Selected bioactive compounds and drugs containing α-amino acids. **b** Nickel-catalyzed enantioconvergent cross-coupling of racemic α-haloglycine derivatives with alkylzinc reagents. **c** Cobalt-catalyzed asymmetric reductive alkylation of dehydroglycine derivatives with alkyl halides. **d** Racemic synthesis of α-amino carbonyls with dihydropyridines. **e** Diastereoselective addition of carbamoyl anions to chiral imines. **f** Catalytic asymmetric synthesis of chiral α-amino amides from formamides, aldehydes and amines. TBSOTf *tert*-butyldimethylsilyltrifluoromethanesulphonate, LDA lithium diisopropylamide, CPA chiral phosphoric acid, HAT hydrogen atom transfer.

haloglycine derivatives with alkylzinc reagents (Fig. 1b), and cobalt-catalyzed asymmetric reductive alkylation of dehydroglycine derivatives with alkyl halides (Fig. 1c) have demonstrated the potential of radical chemistry to overcome limitations of traditional approaches[24–26], albeit that pre-prepared substrates with specific activation groups are still required. Among various radical species, carbamoyl radicals are particularly attractive for amino acid synthesis due to their nucleophilic character and potential for direct amide bond formation[27]. However, prevalent strategies for harnessing carbamoyl radicals typically rely on 4-substituted-1,4-dihydropyridines (DHPs) as precursors[28–30], requiring multi-step synthesis and offering limited substrate scope, albeit that the generation of carbamoyl radicals from formamides via hydrogen atom transfer (HAT) is known for racemic Minisci-type carbamoylations[31,32] and hydrocarbamoylations[33]. The most recent approach employs visible light and Lewis acid activation of DHPs to generate carbamoyl radicals for three-component reactions with in situ-formed imines or iminiums[34], yet asymmetric variants remain undeveloped (Fig. 1d). Alternative strategies using simple formamides as carbamoyl anion precursors require strong bases (e.g., LDA) and chiral auxiliaries[35], limiting practical applications (Fig. 1e). Thus, a general, catalytic asymmetric strategy to harness carbamoyl radicals from simple formamides for the synthesis of amino acid derivatives remains an unmet challenge.

Herein, we report a dual catalytic system that integrates a HAT-mediated carbamoyl radical generation with a stereocontrolled ionic and H-bonding activated asymmetric addition between carbamoyl radical and an in situ formed imine. This strategy enables rapid and modular assembly of α-amino amides from readily available aldehydes,

Table 1 | Optimization of the Reaction[a]

1	**without 5**	**25**	**10 W**	**0.25/0.5**	**81**	**-**
2	**5a**	25	10 W	0.25/0.5	38	6
3	**5b**	25	10 W	0.25/0.5	44	37
4	(*R*)-Na[**5b**]	25	10 W	0.25/0.5	93	38
5	(*R*)-K[**5b**]	25	10 W	0.25/0.5	98	37
6	(*R*)-Ca[**5b**]$_2$	25	10 W	0.25/0.5	46	27
7	(*R*)-Cs[**5b**]	25	10 W	0.25/0.5	79	38
8	(*R*)-Na[**5c**]	25	10 W	0.25/0.5	99	43
9	(*R*)-Na[**5c**]	25	10 W	0.25/1.0	82	43
10	(*R*)-Na[**5c**]	25	10 W	0.5/0.5	99	26
11	(*R*)-Na[**5c**]	−30	10 W	0.25/0.5	92	68
12	(*R*)-Na[**5c**]	−30	40 W	0.25/0.5	99	74
13	(*R*)-Na[**5c**]	−78	40 W	0.25/0.5	58	93
14[d]	(*R*)-Na[**5c**]	−78	40 W	0.25/0.5	85	96
15[d]	**5c**	−78	40 W	0.25/0.5	67	95
16[de]	(*R*)-Na[**5c**]	−78	40 W	0.25/0.5	75	91

Cy cyclohexyl, *TBADT* tetrabutylammonium decatungstate, *TMP-NH$_2$* 3,4,5-trimethoxyaniline, *MeCN* acetonitrile, *DCM* dichloromethane.
[a]Reaction conditions: Unless indicated otherwise, the reaction of **1a** (0.05 mmol), **2a** (0.1 mmol), and **3a** (0.125 mmol) was carried out in MeCN/DCM at room temperature in the presence of TBADT (9 mol%) and **5** (20 mol%) under irradiation with a 10 W 390 nm LED.
[b]Isolated yield.
[c]The ee values were determined by HPLC analysis.
[d]Reaction time was extended to 48 h.
[e]Na[**5c**] was used at 10 mol% loading.

amines, and formamides (Fig. 1f). We sort out the cumulative challenges that compatibility among the individual species in the reaction mixture (catalysts, substrates, intermediates), side reactions, catalyst deactivation, realization of broad substrate scope. The developed protocol affords a wide range of α-amino amide derivatives (>80 examples) with up to >99% yield and >99% enantioselectivity.

Results

Reaction optimization

We initiated our investigation with a reaction of *N-tert*-butylformamide (**1a**), cyclohexanecarbaldehyde (**2a**), and 3,4,5-trimethoxyaniline (**3a**, TMP-NH$_2$) to synthesize chiral α-amino amide **4a**. Tetrabutylammonium decatungstate (TBADT), a well-established hydrogen atom transfer (HAT) catalyst[36,37], was selected to generate a carbamoyl radical from formamide **1a** under irradiation with a 10 W 390 nm LED at room temperature. This nucleophilic radical was anticipated to undergo addition to the in situ formed imine, affording product **4a**. Initial experiments conducted without a Brønsted acid co-catalyst[38,39] yielded the desired product in 81% yield, albeit in racemic form (Table 1, entry 1). Although the introduction of chiral phosphoric acid **5a** only induced 6% ee (entry 2), employing the more sterically demanding TRIP catalyst (**5b**) significantly improved enantioselectivity to 37% ee, suggesting that the chiral Brønsted acids could control the stereochemical outcome by activating the imine substrate (entry 3). The enhanced enantioselectivity likely results from more effective facial discrimination of the imine intermediate due to the increased steric bulk around the active site.

We then explored the effect of various counterions by evaluating the corresponding phosphate salts (entries 4–7). The sodium salt catalyst exhibited the most promising results in terms of both yield and enantioselectivity. We hypothesize that the sodium cation provides an optimal balance of Lewis acidity for imine activation while maintaining appropriate solubility and catalyst conformation[40,41]. Modification of the 3,3′-position on the BINOL backbone from TRIP to 2,4,6-tricyclopentylphenyl substituents (Na[**5c**]) afforded quantitative yield with slightly enhanced enantioselectivity (entry 8 vs. entry 4), supporting our strategy of tuning the chiral pocket's steric environment. Further optimization of reaction parameters revealed that the solvent composition and ratio (MeCN:DCM) substantially influenced both yield and enantioselectivity (entries 9–10). This solvent effect likely stems from changes in the imine formation equilibrium and the organization of the transition state assembly. Lowering the reaction temperature to −30 °C considerably improved enantioselectivity to 68% (entry 11). Increasing the light source power to 40 W further enhanced the ee to 74% (entry 12). When the reaction was conducted at −78 °C, the enantioselectivity increased dramatically to 93% ee, albeit with diminished yield (58%, entry 13). Extending the reaction time to 48 h at −78 °C proved optimal, furnishing product **4a** in 85% yield with excellent enantioselectivity (96% ee, entry 14). Chiral Brønsted acid **5c** instead of its sodium salt provided the product with diminished yield and similar enantioselectivity (67%, 95% ee; entry 15 vs. entry 14). Notably, reducing the sodium chiral phosphate catalyst loading to 10 mol% (entry 16) resulted in only slightly diminished yield and enantioselectivity, indicating that lower catalyst loadings remain viable for practical applications.

Substrate scope

Having established optimal reaction conditions, we proceeded to explore the substrate scope of this transformation. We began by investigating various formamide derivatives while maintaining cyclohexanecarbaldehyde (**2a**) and 3,4,5-trimethoxyaniline (**3a**) as standard coupling partners (Fig. 2). The optimized conditions proved effective across a diverse range of formamides. Primary formamide was also tolerated, affording product **4b** in 95% yield, albeit with lower enantioselectivity (73% ee) compared to **4a**, suggesting that increased steric bulk on the formamide might be beneficial for enantiocontrol. Under this guidance, we found *N*-methyl (**4c**), *N*-ethyl (**4d**), *N*-isopropyl (**4e**) and other formamides (**4f, 4g**) were well-tolerated, delivering the desired products in moderate to excellent yields (53-91%) and higher enantioselectivities (83-93% ee). Notably, the reaction accommodated formamides bearing cyclic motifs of varying ring sizes. The cyclopropyl derivative **4h** (96% yield, 65% ee) and cyclohexyl derivative **4i** (98% yield, 93% ee) were obtained in excellent yields, though with some variation in enantioselectivity. Sterically demanding formamides (**4j, 4k**) afforded the corresponding products in lower yields but maintained good stereoselectivity. *N*-Aryl formamide could also undergo the reaction, albeit with lower yield and enantioselectivity (**4l**). We next examined the scope with respect to the aniline component. Aniline (**4m**) and *para*-substituted anilines bearing various functional groups including F (**4n**), Cl (**4o**), Br (**4p**), Me (**4q**), OMe (**4r**), and OPMP (**4 s**) were all compatible with the reaction conditions, furnishing products in generally high yields (68-98%) and excellent enantioselectivities (82-95% ee). *Meta*-substituted anilines (**4t-4y**) displayed similar reactivity, with yields ranging from 63% to 78% and consistently high enantioselectivities (88–94% ee). *Ortho*-substituted anilines were not tolerated, probably due to steric effect. The formamides derived from secondary amines (e.g., DMF) could not undergo the reaction (Please see Supplementary Information for details, Page S54). The methodology also accommodated more elaborate substitution patterns, as exemplified by products **4z-4ad** (67–93% yield, 80–94% ee).

Having established the broad compatibility of formamides and anilines, we next explored the scope with respect to the aldehyde components (Fig. 3). Cyclic aliphatic aldehydes performed exceptionally well, with cyclopentyl (**6a**) and 4,4-difluoro-cyclohexyl (**6b**) derivatives providing high yields (88-99%) and excellent enantioselectivities (93–95% ee). Aldehydes derived from tetrahydropyran (**6c**) and *N*-Boc piperidine (**6d**) maintained high stereoselectivity (94–98% ee). Other aliphatic aldehydes (**6e-6l**), including simple unbranched and variously branched structures, consistently delivered the desired products with high enantioselectivities (78–92% ee). Notably, the

https://doi.org/10.1038/s41467-025-68073-w

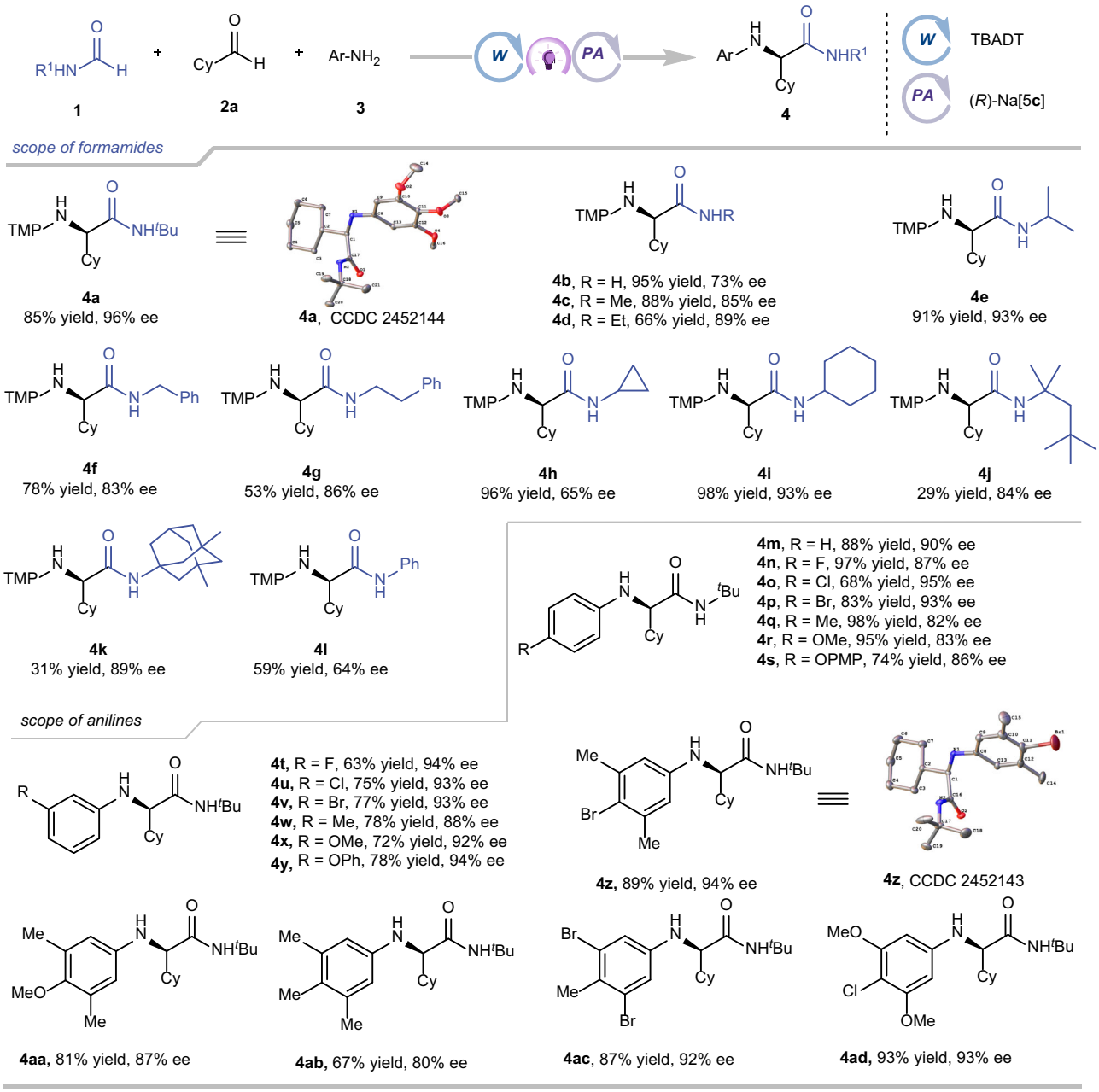

Fig. 2 | Substrate scope of formamides and anilines. Reaction conditions: The reaction of **1** (0.05 mmol), **2a** (0.1 mmol) and **3** (0.125 mmol) was carried out in MeCN (0.25 mL) and DCM (0.5 mL) in the presence of TBADT (9 mol%), (*R*)-Na[**5c**] (20 mol%) under 40 W 390 nm LED light at −78 °C for 48 h. PMP 4-methoxyphenyl, Ph phenyl.

protocol accommodated diverse functional groups including alkenes (**6 m**), alkynes (**6n**), halogens (**6o, 6p**), and protected functionalities (**6q, 6r**), providing orthogonal functionalities for subsequent molecular assembly, all delivering products with good stereoselectivity (86–94% ee). Aliphatic aldehydes with aromatic substituents, **6s**-**6u**, also delivered high enantioselectivities (85–90% ee). Aromatic aldehydes could also undergo the reaction, albeit with much lower yield and enantioselectivity, e.g., benzaldehyde (**Ar-TM**, 46%, 37% ee). α-Substituted racemic aldehydes (**6v**-**6x**) afforded β-branched non-canonical amino acid derivatives, valuable molecules in modern drug development efforts[42], with up to 8:1 diastereoselectivities and moderate to high enantioselectivities (71–85% ee). These products exhibited *syn*-selectivity, which aligns well with the Felkin-Anh model[43] for α-substituted imines[44,45], as shown in **TS-1**. The methodology could also be applied to more complex substrates. For example, oleic aldehyde (**6y**), aldehyde derived from erucic acid (**6z**), citronellal (**6aa**), and cyclamen aldehyde (**6ab**) were successfully transformed with good stereoselectivity (78–92% ee/de). The methodology's compatibility with bioactive molecule-derived components was demonstrated through the successful incorporation of orlistat (**6ac**) and dopamine (**6ad**) moieties, underlining potential applications in medicinal chemistry and late-stage functionalization.

To demonstrate the broader utility of our methodology, we extended its application to more structurally complex and biologically important targets, including α,β-diamino amides[46,47], glycosylated amino acids[48], and peptides (Fig. 4). First, the reaction was applied to chiral *N*-Boc α-amino aldehydes for synthesizing α,β-diamino amides. Under standard conditions, the aldehyde derived from *L*-phenylalanine afforded the corresponding *syn*-α,β-diamino amide *syn*-**7a** with excellent diastereoselectivity, 38% yield and 98% ee. Interestingly, conducting the reaction at −30 °C without the chiral sodium phosphate catalyst still provided *syn*-**7a** with 34% yield and 93% ee. This high

https://doi.org/10.1038/s41467-025-68073-w

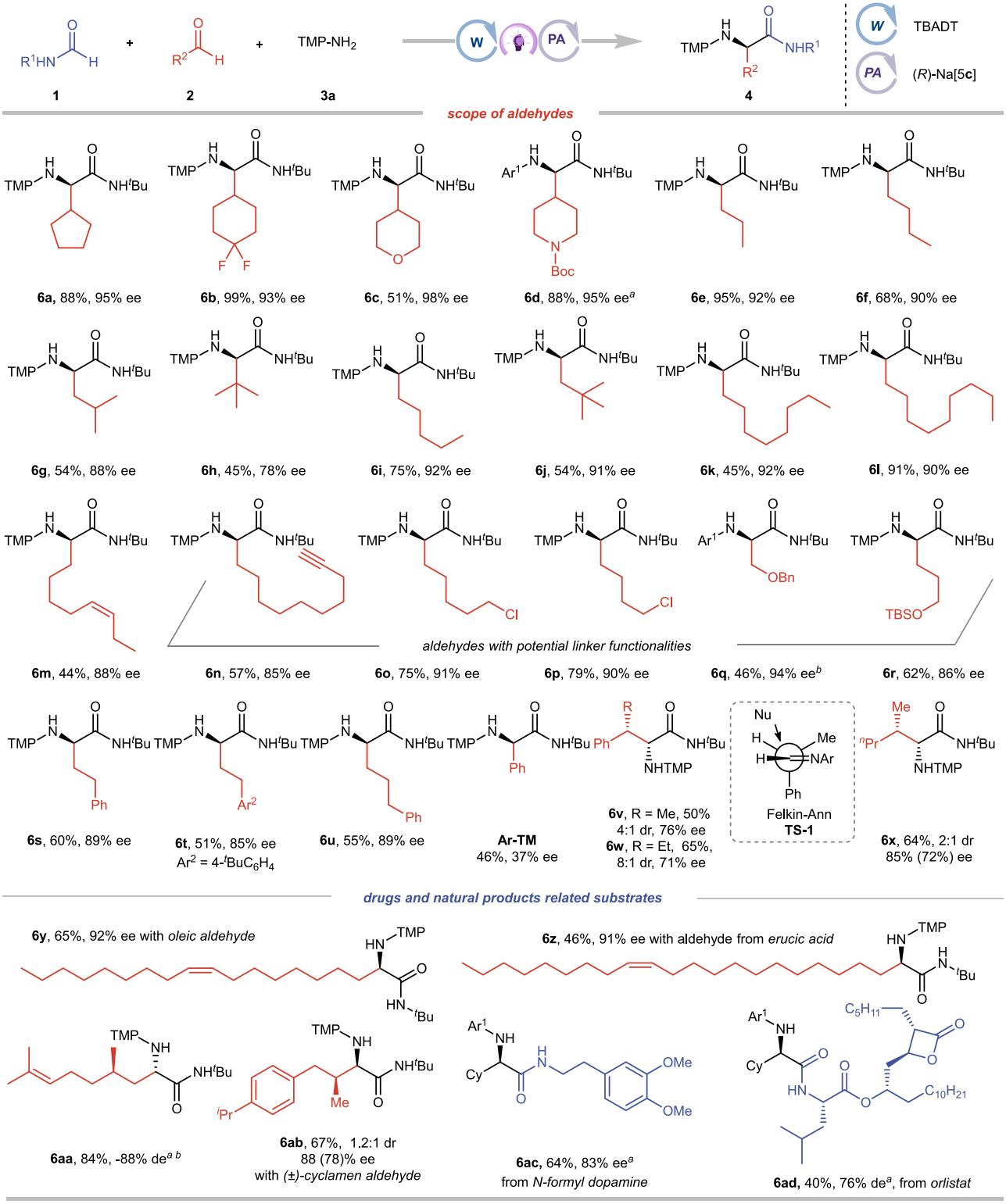

Fig. 3 | Substrate scope of aldehydes, drugs and natural products related substrates. Reaction conditions: The reaction of **1a** (0.05 mmol), **2** (0.1 mmol) and **3a** (0.125 mmol) was carried out in MeCN (0.25 mL) and DCM (0.5 mL) in the presence of TBADT (9 mol%), (*R*)-Na[**5c**] (20 mol%) under 40 W 390 nm LED light at −78 °C for 48 h. [a]Reaction conditions: The reaction of **1** (0.25 mmol), **2** (0.1 mmol) and **3b** (0.125 mmol) was carried out in MeCN (0.25 mL) and DCM (0.5 mL) in the presence of TBADT (4.5 mol%), (*R*)-Na[**5c**] (20 mol%) under 40 W 390 nm LED light at −78 °C for 48 h. [b](*S*)-Na[**5b**] was used. Ar^1 4-bromo-3,5-dimethylphenyl, Ar^2 4-(*tert*-butyl)phenyl.

https://doi.org/10.1038/s41467-025-68073-w

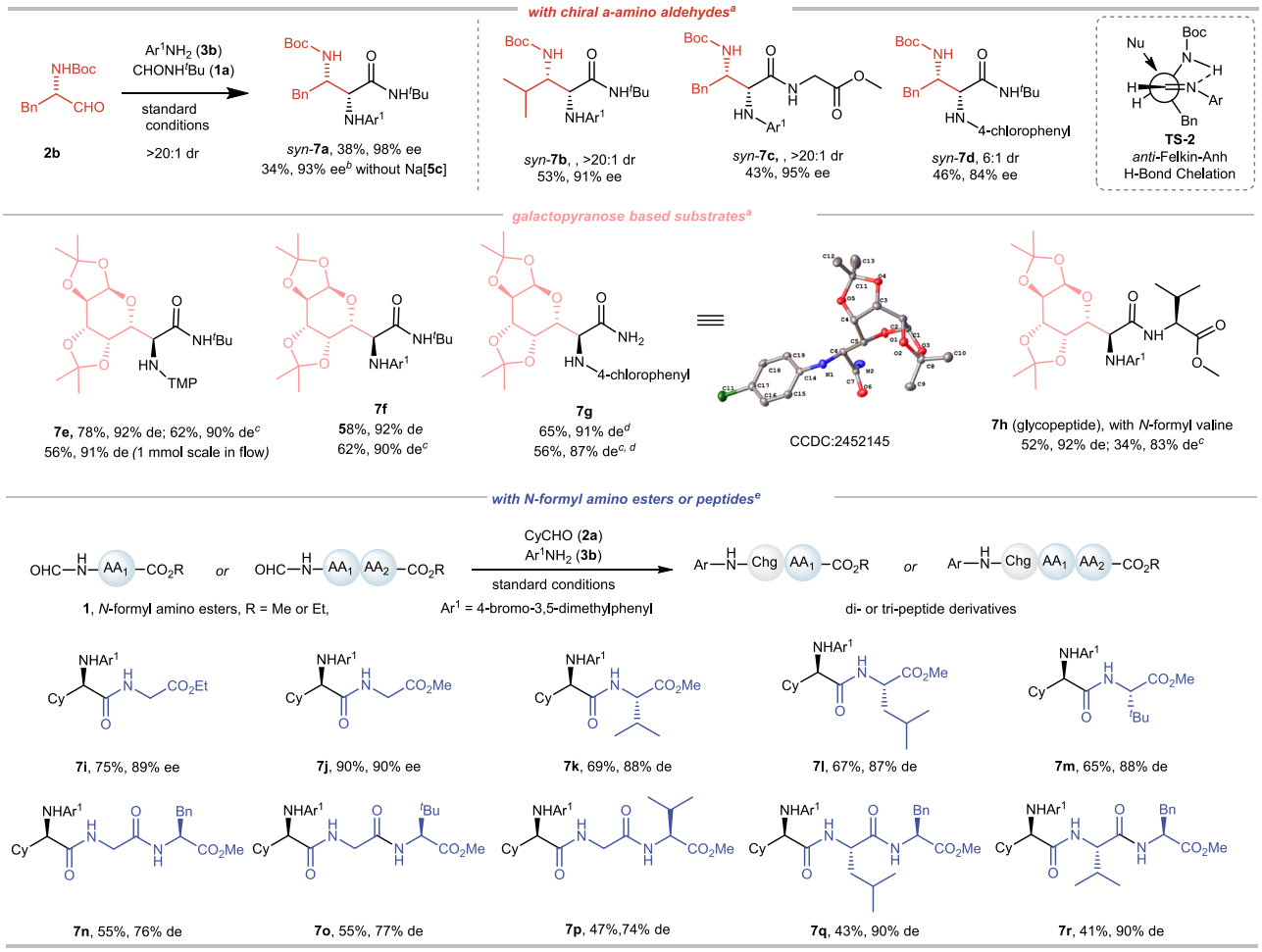

Fig. 4 | Scope of *a*-amino aldehydes, galactopyranose based and peptides related substrates. [a]Reaction conditions: The reaction of **1** (0.25 mmol), **2** (0.1 mmol) and **3** (0.125 mmol) was carried out in MeCN (0.5 mL), DCM (1.0 mL) in the presence of TBADT (4.5 mol%), (*R*)-Na[**5c**] (20 mol%) under 40 W 390 nm LED light at −78 °C for 96 h. [b]**7a** was synthesized without CPA-Na at −30 °C. [c]Without CPA-Na. [d]The de was determined by ^{1}H NMR while other products were determined by ^{1}H NMR and HPLC. [e]Reaction conditions: The reaction of **1** (0.25 mmol), **2a** (0.1 mmol) and **3b** (0.125 mmol) was carried out in MeCN (0.5 mL), DCM (1.0 mL) in the presence of TBADT (4.5 mol%), (*R*)-Na[**5c**] (20 mol%) under 40 W 390 nm LED light at −78 °C for 96 h. Ar^1 4-bromo-3,5-dimethylphenyl, Boc *tert*-butyloxycarbonyl, Bn benzyl.

intrinsic diastereoselectivity likely originates from substrate control[49], and the *anti*-Felkin-Anh selectivity could be attributed to **TS-2**, featuring an intramolecular hydrogen bond between the Boc-*N*-H and the imine. Analogous behavior was observed in the aldol-type reaction of *N*-Boc α-amino aldehydes[50]. The temperature-dependent erosion of the ee is attributed to partial racemization of the chiral aldehyde (Supplementary Table S2). High diastereoselectivity (>20:1 dr) and excellent enantioselectivity (>90% ee) were consistently observed for other *N*-Boc α-amino aldehydes, yielding products **7b** and **7c**. The protocol also proved effective in carbohydrate chemistry, converting galactopyranose-derived aldehydes into complex glycosylated amino acid derivatives (**7e**-**7g**) and glycopeptide **7h** with high diastereoselectivity. Consistent with the α-amino aldehyde results, significant substrate-induced diastereocontrol was observed, allowing for high selectivity even without the chiral catalyst. The absolute and relative configuration of **7g** was unambiguously determined by single-crystal X-ray analysis. Furthermore, the methodology was successfully applied to peptide synthesis—a critical area in chemical biology and medicinal chemistry[51]—by employing *N*-formyl amino esters or peptides. This approach generated a series of dipeptides (**7i**-**7m**) in good to excellent yields (65–90%) with high levels of stereoselectivity (89-90% ee for achiral formylglycinate; 87–88% de for chiral *N*-formyl amino esters). The method proved compatible with diverse amino acid side chains, as exemplified by glycine (**7i, 7j**), valine (**7k**), leucine (**7l**) and *tert*-leucine (**7m**). Notably, for these substrates, the diastereoselectivity appeared to be primarily governed by the chiral catalyst rather than the substrate's stereocenter (**7a**-**7h**), likely due to the greater distance between the existing chiral center and the reacting prochiral imine (Please see Supplementary Information for details, Page S52). This strategy was readily extended to tripeptide synthesis, furnishing derivatives **7n**-**7r** with high diastereoselectivities (74–90% de) using *N*-formyl dipeptides as precursors.

The practical utility and scalability of our protocol were demonstrated by conducting the synthesis of α-amino amides **4a** and **4z** on a 1.0 mmol scale, achieving good yields (70 (64)% and 68%, respectively) and high enantioselectivities (94 (84)% and 93% ee) (Fig. 5a). Albeit with slightly lower yield and ee, a significant improvement in reaction efficiency was realized in flow (e.g., 1 mmol scale of **4a** prepared in around 3.8 h in flow vs. 72 h in batch). Importantly, these amide products could be efficiently converted into the valuable free α-amino acids. For instance, **4a** and **4z** underwent a two-step sequence involving oxidative removal of the arylamine moiety using TCCA/HCl[52], followed by *tert*-butylamide hydrolysis with 6 M HCl, to afford the corresponding free amino acids **8** (95% yield, 91% ee from **4a**; 90% yield from **4z**) with minimal erosion of stereochemical integrity. Furthermore, the method readily facilitates the incorporation of isotopic labels (Fig. 5b). Using

https://doi.org/10.1038/s41467-025-68073-w

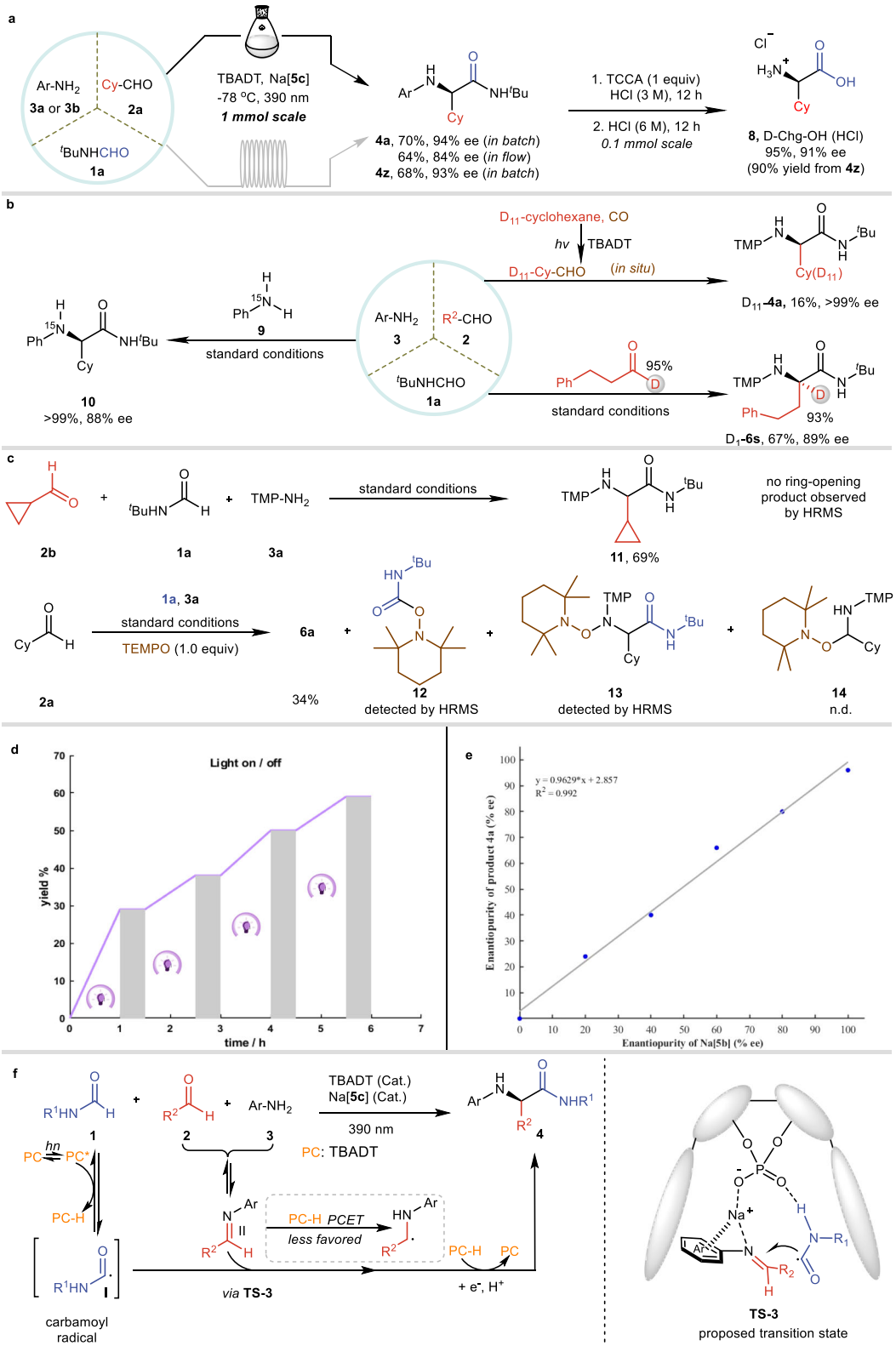

Fig. 5 | The practical utility and mechanism studies of the reaction. a 1.0 Mmol scale reactions. **b** The incorporation of isotopic labels. **c** Control experiments. **d** Light on-off experiments. **e** Linear effect study. **f** Proposed mechanism. TCCA trichloroisocyanuric acid, HRMS High-Resolution Mass Spectrometry, Cy cyclohexyl, TBADT tetrabutylammonium decatungstate, TMP-NH_2 3,4,5-trimethoxyaniline, PCET proton-coupled electron transfer.

^{15}N-labeled aniline (**9**) yielded the ^{15}N-containing amino amide **10** with excellent conversion and high enantioselectivity (88% ee). Access to α-deuterated derivatives was demonstrated using D_1-3-phenylpropanal, providing D_1-**6s** in 67% yield and 89% ee. Showcasing compatibility with in situ generated substrates, D_{11}-cyclohexanecarbaldehyde—prepared via TBADT-photocatalyzed carbonylation[53,54] of D_{12}-cyclohexane under CO atmosphere and light irradiation—was directly utilized in the three-component reaction to furnish the heavily deuterated product D_{11}-**4a** (16%, >99% ee). These results underscore the methodology's robustness, scalability, and adaptability for preparing structurally diverse and isotopically labeled amino acid derivatives.

Proposed mechanism

To gain insight into the reaction mechanism, several control experiments were conducted (Fig. 5c–f). Subjecting cyclopropanecarbaldehyde (**2b**) to the standard conditions afforded the corresponding α-amino amide **11** in 65% yield, with no evidence of cyclopropane ring-opening. This suggests that the reaction likely proceeds via the addition of a relatively nucleophilic radical intermediate[55], avoiding intermediates prone to inducing ring-opening. The involvement of radical species was further substantiated by adding the radical scavenger TEMPO (1.0 equiv) to the standard reaction involving cyclohexanecarbaldehyde **2a**. This resulted in a significantly decreased yield of the desired product **6a** (34%) and the detection by HRMS of the TEMPO adduct of the carbamoyl radical (**12**) as well as the adduct (**13**) derived from trapping the subsequent α-amino radical intermediate formed after C-C bond formation. Conversely, species **14**, potentially arising from single-electron reduction of the imine intermediate, was not detected. Additionally, light on/off experiments demonstrated that product formation ceased in the dark and resumed upon re-irradiation, confirming the reaction's dependence on light energy and suggesting a photocatalytic process rather than a self-sustaining radical chain mechanism (Fig. 5d). We conducted an experiment to investigate the relationship between the ee of Na[**5b**] and the ee of product **4a**. A linear correlation was observed, suggesting that a single molecule of the Na[**5b**] catalyst is involved in the enantiodetermining step (Fig. 5e). Based on these experimental findings and relevant literature[56–59],we propose a plausible catalytic cycle (Fig. 5f). Initially, visible light excitation of the photocatalyst TBADT (PC) generates its excited state (PC*). This excited state abstracts a hydrogen atom (HAT) from formamide **1** to produce the key carbamoyl radical intermediate (**I**) and the reduced form of photocatalyst (PC-H). Concurrently, aldehyde **2** and amine **3** reversibly condense to form imine **II**. The chiral sodium phosphate catalyst (Na[**5c**]) then coordinates to, activates and stabilize imine **II**, setting the stage for the enantioselective addition of the carbamoyl radical **I**. This forms a transient α-amino radical species which, upon subsequent oxidation (likely involving PC-H regenerating PC) and protonation, yields the final α-amino amide product **4** and finishes the catalytic cycle. We propose transition state **TS-3** to describe the enantioselective addition of carbamoyl radical **I**. The chiral sodium phosphate catalyst plays a multifunctional role: (i) Na^+ acts as a Lewis acid to activate the imine intermediate; (ii) Na^+ stabilizes the transition state via cation–π interactions; and (iii) the P = O moiety serves as a hydrogen bond acceptor for the formamide N–H, which increases electron density on the nitrogen and thereby enhances the nucleophilicity of the carbamoyl radical. This proposed hydrogen bonding interaction is supported by the observation that formamides derived from secondary amines, which lack the N–H bond, failed to yield the desired products (see Supplementary Information, pages S54 and S69).

Discussion

In conclusion, we have established a highly enantioselective photoredox protocol employing a dual catalytic system of TBADT and a chiral sodium phosphate. This method enables the direct assembly of valuable chiral α-amino amides from simple, readily available aldehydes, amines, and formamides, circumventing the need for substrate pre-functionalization. The broad utility was showcased by synthesizing structurally diverse targets, including α,β-diamino acids, glycosylated derivatives, and peptides with excellent stereocontrol. Furthermore, facile conversion to free amino acids, amenability to isotopic labeling, and demonstrated scalability underscore the practicality of this approach, offering a powerful platform for accessing diverse chiral scaffolds relevant to peptide science and medicinal chemistry.

Methods

General procedure for the synthesis of chiral amino acid derivatives

A flame-dried 10 mL Schlenk tube was charged with aniline **3** (0.125 mmol, 2.5 equiv), TBADT (0.0045 mmol, 9 mol%), and (*R*)-Na[**5c**] (0.010 mmol, 20 mol%). The vessel was subjected to three cycles of evacuation and backfilling with N_2. Then, MeCN, DCM, **1** (0.05 mmol, 1.0 equiv), and **2** (0.1 mmol, 2.0 equiv) were added. The resulting mixture was frozen in liquid nitrogen, and the headspace was evacuated. The resulting solution was stirred under LED (390 nm 40 W) at −78 °C for 48 h. After completion, the mixture was removed from irradiation and concentrated under reduced pressure. Purification by silica gel chromatography (petroleum ether/ethyl acetate) afforded the target products.

Data availability

Crystallographic data for the structures reported in this Article have been deposited at the Cambridge Crystallographic Data Center, under deposition numbers CCDC 2452144 (**4a**), 2452143 (**4z**) and 2452145 (**7g**). Copies of the data can be obtained free of charge via https://www.ccdc.cam.ac.uk/structures/. Full experimental procedures and the data supporting the findings of this study are available within the article and its Supplementary Information. All data are available from the corresponding author upon request.

References

1. Loredano, P. & Stefano, S. *Unnatural Amino Acids* (Springer, New York, 2012).
2. Wenger, R. M. Synthesis of cyclosporine and analogues: structural requirements for immunosuppressive activity. *Angew. Chem. Int. Ed.* **24**, 77–85 (1985).
3. Richter, H. G. F. et al. Discovery of novel and orally active FXR agonists for the potential treatment of dyslipidemia & diabetes. *Bioorg. Med. Chem. Lett.* **21**, 191–194 (2011).
4. Perucca, E., Yasothan, U., Clincke, G. & Kirkpatrick, P. Lacosamide. *Nat. Rev. Drug Discov.* **7**, 973–974 (2008).
5. Gounder, M. et al. Nirogacestat, a γ-secretase inhibitor for desmoid tumors. *New Engl. J. Med.* **388**, 898–912 (2023).
6. Jarvo, E. R. & Miller, S. J. Amino acids and peptides as asymmetric organocatalysts. *Tetrahedron* **58**, 2481–2495 (2002).
7. Huang, Y., Wiedmann, M. M. & Suga, H. RNA display methods for the discovery of bioactive macrocycles. *Chem. Rev.* **119**, 10360–10391 (2019).
8. Frankel, A., Li, S., Starck, S. R. & Roberts, R. W. Unnatural RNA display libraries. *Curr. Opin. Struct. Biol.* **13**, 506–512 (2003).
9. Najera, C. & Sansano, J. M. Catalytic asymmetric synthesis of alpha-amino acids. *Chem. Rev.* **107**, 4584–4671 (2007).
10. Saghyan, A. S. & Langer, P. *Asymmetric Synthesis of Non-Proteinogenic Amino Acids* (Wiley-VCH, 2016).
11. Ratovelomanana-Vidal, V., Phansavath, P., Ponra, S. & Boudet, B. Recent developments in transition-metal-catalyzed asymmetric hydrogenation of enamides. *Synthesis* **53**, 193–214 (2020).
12. Abdine, R. A. A., Hedouin, G., Colobert, F. & Wencel-Delord, J. Metal-catalyzed asymmetric hydrogenation of C=N bonds. *ACS Catal.* **11**, 215–247 (2020).

13. Hu, L., Wang, Y. Z., Xu, L., Yin, Q. & Zhang, X. Highly enantioselective synthesis of N-unprotected unnatural alpha-amino acid derivatives by ruthenium-catalyzed direct asymmetric reductive amination. *Angew. Chem. Int. Ed.* **61**, e202202552 (2022).
14. Smith, A. M. R. & Hii, K. K. Transition metal catalyzed enantioselective α-heterofunctionalization of carbonyl compounds. *Chem. Rev.* **111**, 1637–1656 (2011).
15. Maruoka, K. & Ooi, T. Enantioselective amino acid synthesis by chiral phase-transfer catalysis. *Chem. Rev.* **103**, 3013–3028 (2003).
16. Li, G. et al. Asymmetric bimetallic catalysis enabled alkenyl *Z*/*E* mutual isomerization. *J. Am. Chem. Soc.* **147**, 20359–20371 (2025).
17. Li, P. et al. Stereodivergent access to non-natural α-amino acids via enantio- and *Z*/*E*-selective catalysis. Science **385**, 972–979 (2024).
18. Eftekhari-Sis, B. & Zirak, M. α-Imino esters in organic synthesis: recent advances. *Chem. Rev.* **117**, 8326–8419 (2017).
19. Zhang, J. et al. Asymmetric phosphoric acid-catalyzed four-component Ugi reaction. *Science* **361**, eaas8707 (2018).
20. Ye, C. X., Shen, X., Chen, S. & Meggers, E. Stereocontrolled 1,3-nitrogen migration to access chiral alpha-amino acids. *Nat. Chem.* **14**, 566–573 (2022).
21. Ye, C.-X., Dansby, D. R., Chen, S. & Meggers, E. Expedited synthesis of α-amino acids by single-step enantioselective α-amination of carboxylic acids. *Nat. Synth.* **2**, 645–652 (2023).
22. Chatgilialoglu, C. & Studer, A. *Encyclopedia of Radicals in Chemistry*, *Vol. 2*: *Synthetic Strategies and Applications*, (John Wiley & Sons, 2012).
23. Nagib, D. A. Asymmetric catalysis in radical chemistry. *Chem. Rev.* **122**, 15989–15992 (2022).
24. Yang, Z. P., Freas, D. J. & Fu, G. C. Asymmetric synthesis of protected unnatural alpha-amino acids via enantioconvergent nickel-catalyzed cross-coupling. *J. Am. Chem. Soc.* **143**, 8614–8618 (2021).
25. Wu, X. et al. Modular alpha-tertiary amino ester synthesis through cobalt-catalysed asymmetric aza-Barbier reaction. *Nat. Chem.* **16**, 398–407 (2024).
26. Zhang, C., Wu, X., Qu, J. & Chen, Y. A general enantioselective alpha-alkyl amino acid derivatives synthesis enabled by cobalt-catalyzed reductive addition. *J. Am. Chem. Soc.* **146**, 25918–25926 (2024).
27. Matsuo, B. T. et al. Photoinduced carbamoylation reactions: unlocking new reactivities towards amide synthesis. *Chem. Commun.* **58**, 8322–8339 (2022).
28. Alandini, N. et al. Amide synthesis by nickel/photoredox-catalyzed direct carbamoylation of (hetero)aryl bromides. *Angew. Chem. Int. Ed.* **59**, 5248–5253 (2020).
29. Cardinale, L., Konev, M. O. & Jacobi von Wangelin, A. photoredox-catalyzed addition of carbamoyl radicals to olefins: a 1,4-dihydropyridine approach. *Chem. Eur. J.* **26**, 8239–8243 (2020).
30. Kim, I., Park, S. & Hong, S. Functionalization of pyridinium derivatives with 1,4-dihydropyridines enabled by photoinduced charge transfer. *Org. Lett.* **22**, 8730–8734 (2020).
31. Quattrini, M. C. et al. Versatile cross-dehydrogenative coupling of heteroaromatics and hydrogen donors via decatungstate photocatalysis. *Chem. Commun.* **53**, 2335–2338 (2017).
32. Kim, I. et al. Site-selective functionalization of pyridinium derivatives via visible-light-driven photocatalysis with quinolinone. *J. Am. Chem. Soc.* **141**, 9239–9248 (2019).
33. Prieto, A. & Taillefer, M. Visible-light decatungstate/disulfide dual catalysis for the hydro-functionalization of styrenes. *Org. Lett.* **23**, 1484–1488 (2021).
34. Liu, J. & Gaunt, M. J. Versatile, modular, and general strategy for the synthesis of α-amino carbonyls. *J. Am. Chem. Soc.* **146**, 24699–24707 (2024).
35. Reeves, J. T. et al. Carbamoyl anion addition to N-sulfinyl imines: highly diastereoselective synthesis of α-amino amides. *J. Am. Chem. Soc.* **135**, 5565–5568 (2013).
36. Tzirakis, M. D., Lykakis, I. N. & Orfanopoulos, M. Decatungstate as an efficient photocatalyst in organic chemistry. *Chem. Soc. Rev.* **38**, 2609–2621 (2009).
37. Ravelli, D., Fagnoni, M., Fukuyama, T., Nishikawa, T. & Ryu, I. Site-selective C–H functionalization by decatungstate anion photocatalysis: synergistic control by polar and steric effects expands the reaction scope. *ACS Catal.* **8**, 701–713 (2018).
38. Akiyama, T. Stronger bronsted acids. *Chem. Rev.* **107**, 5744–5758 (2007).
39. Parmar, D., Sugiono, E., Raja, S. & Rueping, M. Complete field guide to asymmetric binol-phosphate derived bronsted acid and metal catalysis: history and classification by mode of activation; bronsted acidity, hydrogen bonding, ion pairing, and metal phosphates. *Chem. Rev.* **114**, 9047–9153 (2014).
40. Shen, K., Liu, X., Cai, Y., Lin, L. & Feng, X. Facile and efficient enantioselective strecker reaction of ketimines by chiral sodium phosphate. *Chem. Eur. J.* **15**, 6008–6014 (2009).
41. Miró, J. et al. Enantioselective allenoate-claisen rearrangement using chiral phosphate catalysts. *J. Am. Chem. Soc.* **142**, 6390–6399 (2020).
42. Li, F., Yang, L.-C., Zhang, J., Chen, J. S. & Renata, H. Stereoselective synthesis of β-branched aromatic α-amino acids by biocatalytic dynamic kinetic resolution. *Angew. Chem. Int. Ed.* **60**, 17680–17685 (2021).
43. Bartolo, N. D., Read, J. A., Valentin, E. M. & Woerpel, K. A. Reactions of allylmagnesium reagents with carbonyl compounds and compounds with C=N double bonds: their diastereoselectivities generally cannot be analyzed using the Felkin-Anh and chelation-control models. *Chem. Rev.* **120**, 1513–1619 (2020).
44. Cheng, X., Goddard, R., Buth, G. & List, B. Direct catalytic asymmetric three-component Kabachnik–Fields Reaction. *Angew. Chem. Int. Ed.* **47**, 5079–5081 (2008).
45. Cowling, M. P., Jenkins, P. R. & Cooper, K. Asymmetric induction in the addition of Grignard reagents to nitrones. *J. Chem. Soc. Chem. Commun.* **22**, 1503–1504 (1988).
46. Viso, A., Fernández, de la Pradilla, R., García, A. & Flores, A. α, β -Diamino acids: biological significance and synthetic approaches. *Chem. Rev.* **105**, 3167–3196 (2005).
47. Pascal, R., Sola, R. & Jouin, P. Unnatural diamino acid derivatives as scaffolds for creating diversity and as linkers for simplifying screening in chemical libraries. *Methods Enzymol.* **369**, 182–194 (2003).
48. Reily, C., Stewart, T. J., Renfrow, M. B. & Novak, J. Glycosylation in health and disease. *Nat. Rev. Nephrol.* **15**, 346–366 (2019).
49. Merino, P., Lanaspa, A., Merchan, F. L. & Tejero, T. Stereoselective grignard reactions to α-amino nitrones. Synthesis of optically active α-aminohydroxylamines and 1,2-diamines. *Tetrahedron: Asymmetry* **8**, 2381–2401 (1997).
50. Jung, C.-K. & Krische, M. J. Asymmetric induction in hydrogen-mediated reductive aldol additions to α-amino aldehydes catalyzed by rhodium: selective formation of *syn*-stereotriads directed by intramolecular hydrogen-bonding. *J. Am. Chem. Soc.* **128**, 17051–17056 (2006).
51. Wang, L. et al. Therapeutic peptides: current applications and future directions. *Signal Transduction Targeted Ther.* **7**, 48 (2022).
52. Zhao, L. & Li, C.-J. Functionalizing glycine derivatives by direct C=C bond formation. *Angew. Chem. Int. Ed.* **47**, 7075–7078 (2008).
53. Jaynes, B. S. & Hill, C. L. Radical carbonylation of alkanes via polyoxotungstate photocatalysis. *J. Am. Chem. Soc.* **117**, 4704–4705 (1995).
54. Boese, W. T. & Goldman, A. S. Alkane carbonylation photocatalyzed by aromatic ketones under high CO pressure. *Tetrahedron Lett* .**33**, 2119–2122 (1992).
55. Minisci, F., Fontana, F., Coppa, F. & Yan, Y. M. Reactivity of carbamoyl radicals. a new, general, convenient free-radical synthesis of

isocyanates from monoamides of oxalic acid. *J. Org. Chem.* **60**, 5430–5433 (2002).
56. Ding, W.-W. et al. Enantioselective synthesis of β- and α-amino ketones through reversible alkane carbonylation. *Nat. Synth.* **3**, 507–516 (2024).
57. Proctor, R. S. J., Davis, H. J. & Phipps, R. J. Catalytic enantioselective Minisci-type addition to heteroarenes. *Science* **360**, 419–422 (2018).
58. Cocco, E. et al. Stereoselective reactions promoted by alkali metal salts of phosphoric acid organocatalysts. *Chem. Cat. Chem* **16**, e202400328 (2024).
59. Garwood, J. J. A., Chen, A. D. & Nagib, D. A. Radical polarity. *J. Am. Chem. Soc.* **146**, 28034–28059 (2024).

Acknowledgements

This work was supported by the National Key R&D Program of China (2021YFA1500100 for L.-Z.G.) and National Natural Science Foundation of China (22188101 for L.-Z.G., 22471255 for Zhi-Yong Han).

Author contributions

W.-W. D. carried out most of the experimental and data analysis work. Zhi-Yuan He and W.-Y. W contributed in the synthesis of catalysts and synthetic applications work. Zhi-Yong Han and L.-Z. G. designed the reaction and directed the project. The paper was written by Zhi-Yong Han and L.-Z. G. All authors contributed to discussions.

Competing interests

The authors declare no competing interests.

Additional information

Supplementary information The online version contains supplementary material available at https://doi.org/10.1038/s41467-025-68073-w.

Correspondence and requests for materials should be addressed to Zhi-Yong Han or Liu-Zhu Gong.

Peer review information *Nature Communications* thanks Guo-Qiang Xu and the other anonymous reviewer(s) for their contribution to the peer review of this work. A peer review file is available.

Reprints and permissions information is available at http://www.nature.com/reprints

Publisher's note Springer Nature remains neutral with regard to jurisdictional claims in published maps and institutional affiliations.

Open Access This article is licensed under a Creative Commons Attribution-NonCommercial-NoDerivatives 4.0 International License, which permits any non-commercial use, sharing, distribution and reproduction in any medium or format, as long as you give appropriate credit to the original author(s) and the source, provide a link to the Creative Commons licence, and indicate if you modified the licensed material. You do not have permission under this licence to share adapted material derived from this article or parts of it. The images or other third party material in this article are included in the article's Creative Commons licence, unless indicated otherwise in a credit line to the material. If material is not included in the article's Creative Commons licence and your intended use is not permitted by statutory regulation or exceeds the permitted use, you will need to obtain permission directly from the copyright holder. To view a copy of this licence, visit http://creativecommons.org/licenses/by-nc-nd/4.0/.

© The Author(s) 2025